Proc. Nonlinear Water Waves Workshop, Bristol, 11-19, 1991.

Spectral evolution in waves traveling over a shoal

J.A. Battjes[†] *and S. Beji*[††]

Abstract

Nonlinear aspects of breaking and non-breaking waves propagating over a submerged trapezoidal bar have been investigated by laboratory experiments, with special emphasis on the generation of high-frequency energy. Data collected from the measurements are used for computing spectral and bispectral estimates in order to assess the contribution of wave breaking to the spectral evolution, as distinguished from that of the conservative nonlinear interactions. It is found that wave breaking itself, even in the case of plunging breakers, does not play a decisive role in the evolution of the spectral shape, but contributes by simply extracting energy in almost averaged manner. An approach is described to utilize this observation by using a semi-empirical formulation for dissipation due to breaking in conjunction with a weakly nonlinear numerical model.

1. Introduction

Harmonic generation in waves passing over submerged obstacles has long been known both experimentally and theoretically. Jolas (1960) carried out experiments with a submerged shelf of rectangular cross section and observed harmonics of a simple incident wave on the transmission side [1]. A few years later, in nonlinear optics, an analogous phenomenon concerning the transmission of a laser beam through a quartz crystal was explained theoretically by Armstrong *et al.* (1962). At about the same time, Phillips [2] gave the theoretical foundations of *nonlinear resonant interactions* between discrete wave components for deep water waves. Hasselmann (1962-63) extended the theory to the case of a continuous spectrum [3]. Mei and Ünlüata (1971), Tappert and Zabusky (1971), Johnson (1972), and Bryant (1973) made important contributions which further clarified the nonlinear interactions in shallow water waves [1, 4, 5].

Despite these achievements, the incorporation of wave breaking into these models remains basically unsolved. This deficiency severely limits their range of applicability, especially in coastal waters. While for non-breaking waves the generation of high frequency wave energy may entirely be attributed to conservative nonlinear effects, there have been doubts about the role of breaking. Some researchers hypothesized it was the wave breaking that controlled the phenomenon rather than conservative nonlinear interactions [6, 7]. The aim of the ongoing work reported here is to help resolve these questions and to contribute to the development of capabilities for numerical modeling of the most important processes observed.

The organization of the paper is as follows. The next section gives a brief description of the experimental arrangements, the bottom profile, and the wave conditions for the measurements. Section 3 begins with some descriptive features of the experiments. Measured power spectra at selected locations and the corresponding spatial variations of potential energy over the submerged bar are given next. The numerical model is introduced in Section 4 and numerical simulations of nonlinear (non-breaking) random waves are compared with the measurements both in time and in spectral domain. Also, an approach is sketched for predicting the spectral evolution of breaking waves.

[†] *Professor, Dept. of Civil Eng., Delft University of Technology, P.O. Box 5048, 2600 GA, Delft, The Netherlands.*

[††] *Post-doctorate fellow, Dept. of Civil Eng., Delft University of Technology, The Netherlands.*

2. Experiments

In order to assess the contribution of wave breaking to the generation, transfer, and dissipation of high frequency energy observed in the power spectra of waves traveling over submerged bars, tests were performed both for non-breaking and breaking (spilling and plunging) waves.

The experiments were carried out in the wave-flume of the Department of Civil Engineering, Delft University of Technology. The flume is 37.7 m long and 0.8 m wide. In its midsection, a trapezoidal submerged bar was built (see Figure 1.) At the downwave end a gently sloping spending beach was present (from previous experiments). The still-water depth was 0.4 m over the original, horizontal flume bottom and had a minimum of 0.10 m above the bar crest. Periodic and irregular input waves were used, the latter with a JONSWAP-type spectrum and a custom-made, very narrow band spectrum which eliminated effects of high-frequency tail in the input spectrum. Peak frequencies were $f_p=0.4$ Hz and $f_p=1.0$ Hz. Measurements of the free surface elevations were made with parallel-wire resistance gages at 8 different locations as sketched in Figure 1.

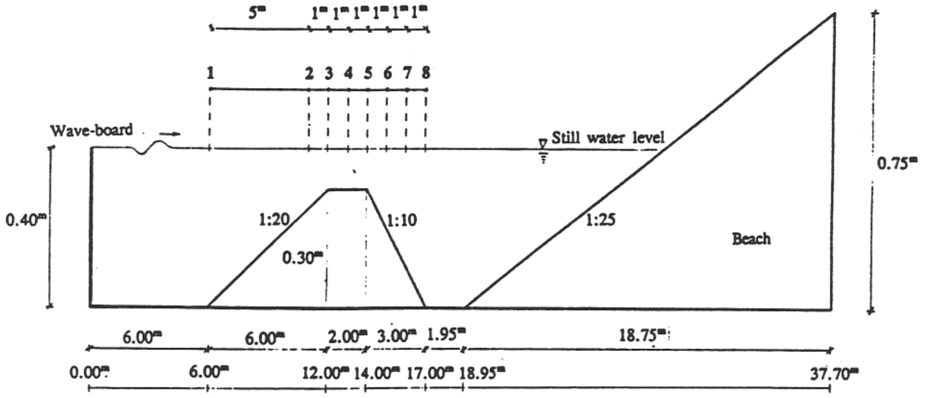

Figure 1 Longitudinal cross-section of wave flume and locations of wave gages.

3. Experimental Results

3.1 Descriptive features

Figures 2a and 2b exhibit the evolutions of the "long" (f=0.4 Hz) and "short" (f=1.0 Hz) waves over topography for monochromatic waves. The records were taken at the stations shown in Figure 1.

The long waves (f=0.4 Hz), once having gained in amplitude, gradually gave rise to one or more waves traveling at nearly the same speed with them in their tails. The evolution continued as the waves propagate over the upslope and horizontal part of the shoal. This phenomenon is reminiscent of the soliton formation behind a solitary wave, a subject which has been studied extensively [8,9]. As these finite amplitude long waves with their accompanying tails moved into the deeper water -downslope- they *decomposed* into several smaller amplitude waves of nearly harmonic frequencies. These released harmonic components then moved at different phase speeds but continued to exchange energy for several wave-lengths; the amplitudes of some of the higher frequency

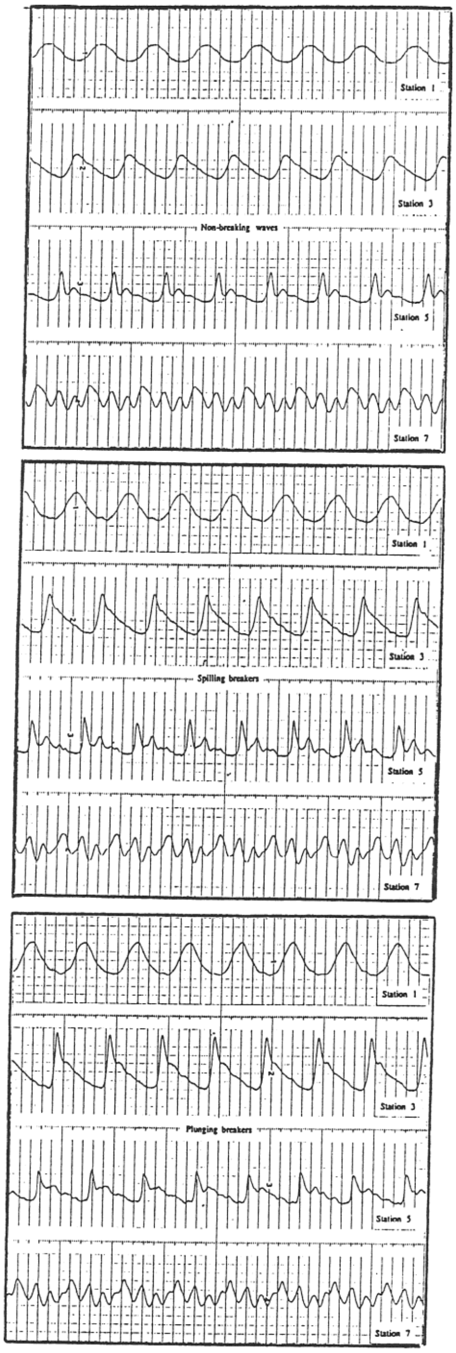

Figure 2a Evolving long waves (T=2.5 s).

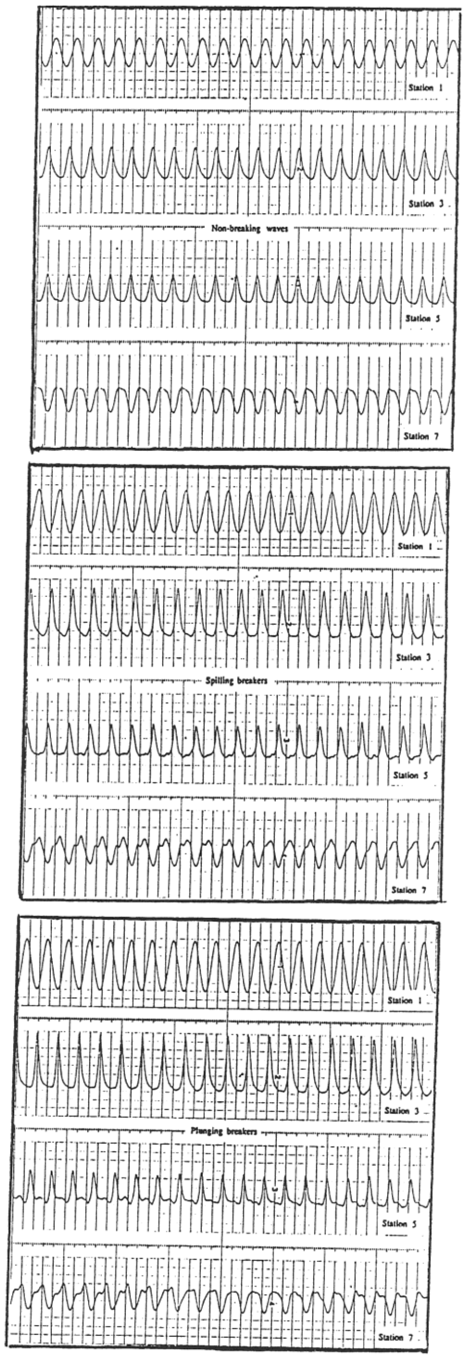

Figure 2b Evolving short waves (T=1.0 s).

components even became larger than that of the primary wave itself.

The short waves ($f=1.0$ Hz), on the contrary, did not develop any tail waves as they grew in amplitude but kept their vertical symmetry and appeared as higher-order Stokes waves. Decomposition in the deeper region was not nearly drastic as that of the longer waves and only relatively smaller amplitude second order harmonics were released.

It is readily seen in the records in Figure 2 that wave breaking does not alter the evolution of the wave forms drastically. From a practical point of view this is encouraging because it implies the possibility of combining a conservative (weakly) nonlinear model, such as a Boussinesq model, with a semi-empirical formulation of the dissipated energy in averaged form. This line of development is pursued presently; preliminary results are given below.

3.2 Spectral evolution

As indicated in Section 2, irregular waves were generated with two different types of spectra. Figure 3 shows the spectral evolutions for the breaking, spilling, and plunging waves ($f_p=0.4$ Hz) at three selected stations for the case of the custom-made narrow band spectrum, for nonbreaking waves, spilling breakers and plunging breakers. It can be observed that the primary wave energy at any given station remains clearly separated from that of the higher frequency part generated by nonlinear interactions. It is important to notice that the overall features of the spectral shape evolution for different wave conditions (nonbreaking or breaking) do not differ appreciably. Further clarification is offered in Figure 4 where the spatial variations of normalized potential energy of the total, the primary, and the higher frequency components are plotted. In computing the primary wave energy the range of integration is taken between 0.0 Hz and 0.6 Hz while for higher frequency energy it is between 0.6 Hz ($= 1\frac{1}{2} f_p$) and 2.5 Hz. The total energy is obtained simply by adding the two. In each case the variations are normalized with respect to the total measured at station 1.

3.3 Bispectral Evolution

Bispectral estimates for a JONSWAP-type incident wave spectrum for non-breaking and plunging waves at selected stations were computed. The results of these computations are outlined below.

In the case of non-breaking waves, at station 3, where the waves enter the shallowest region, primary frequency components interact strongly with themselves, f_p-f_p, and provide a driving mechanism for the generation of the second harmonic components, $2f_p$. At station 5, the second and third harmonic components, $2f_p$ and $3f_p$, grow strong enough to engage in appreciable interactions with the primary waves components, f_p-$2f_p$ and f_p-$3f_p$. Although not as strong, the interactions of the second harmonics with themselves, $2f_p$-$2f_p$, are also visible. At station 7, in the deeper region behind the bar, the strength of the interactions is diminished, and the primary wave component interactions, f_p-f_p, are no longer dominant because the amplitudes of higher frequency waves are now comparable with those of the peak frequency components.

In the case of plunging breakers, at station 3, the nonlinear interactions are already spread to encompass the higher frequencies. This is not surprising because the significant wave height is now 1.7 times greater than its counterpart in the non-breaking case. However, as we move to station 4 we see a sharp decrease -nearly 50%- in the strength of nonlinear interactions. This is a direct consequence of wave breaking: *clipping* wave heights by breaking reduces the degree of nonlinearity. At station 7 the strength of interactions is only a fraction of those in the previous cases but not expended completely. Indeed the significant wave height in this case at this particular station is still

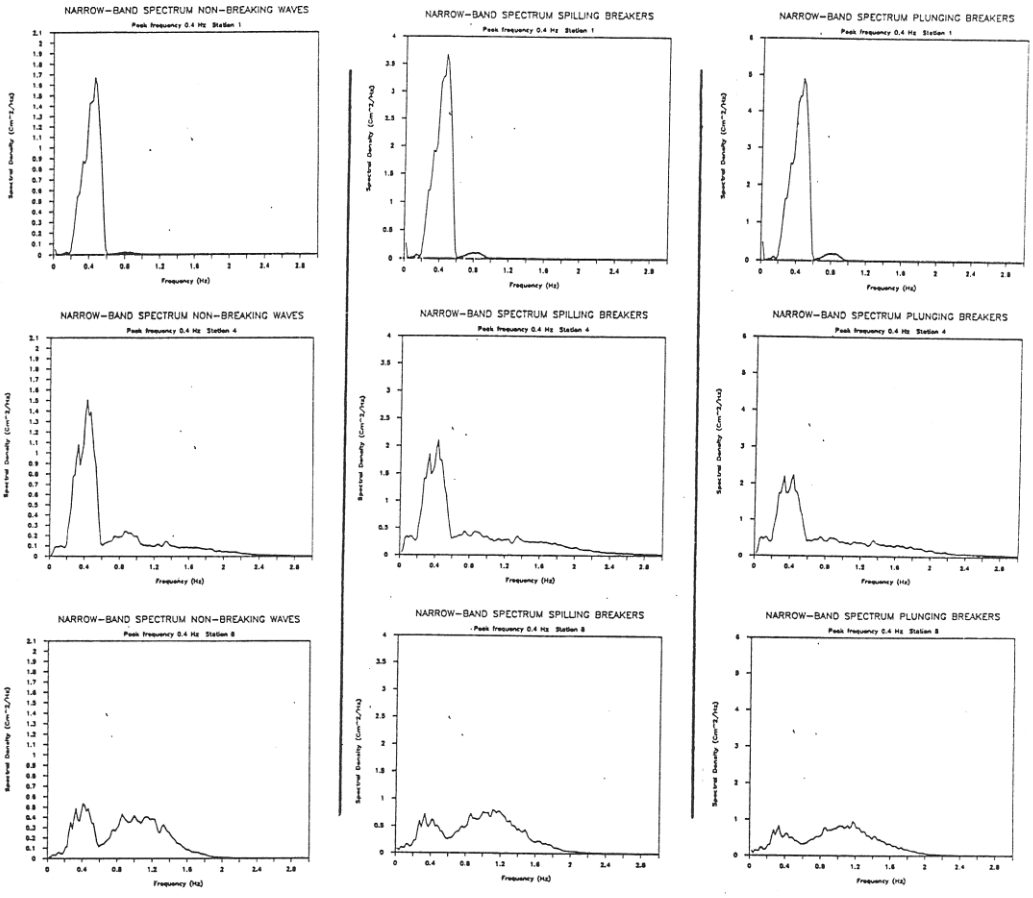

Figure 3 Spectral evolutions for non-breaking, spilling, and plunging waves.

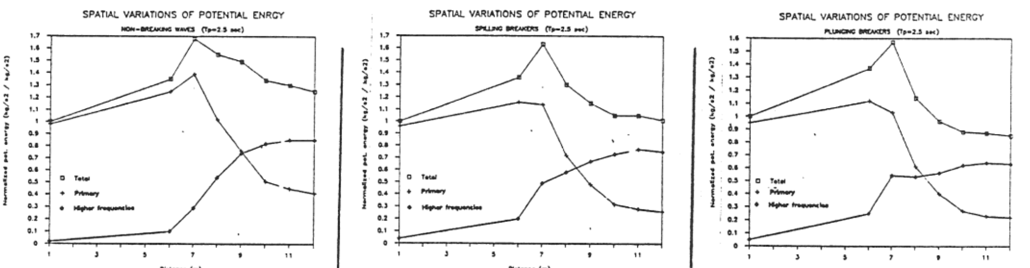

Figure 4 Spatial variations of total potential energy of the primary wave field and of higher frequencies.

1.4 times greater than the one measured for non-breaking waves. The strength of the nonlinear interactions is likewise greater.

4.Numerical modeling

4.1 Introduction

The observation that in our experiments the evolution of the spectral shape is not significantly affected by wave breaking suggests the possibility of using a (non-spectral) model for the dissipation of total wave energy by breaking, in conjunction with a conservative (potential-flow) model incorporating nonlinear wave-wave interactions. This development is in progress.

4.2 Numerical model

As a first step, a conservative nonlinear wave propagation model has to be chosen. "Exact" nonlinear models solving the full governing equations [10] are considered to be too demanding in computational effort in view of the intended operational use (ultimately). Instead, a Boussinesq type model was chosen because it does contain nonlinearity and it is suited for shallow-water conditions. We used it in the following form:

$$u_t + uu_x + g\zeta_x = \frac{1}{3}h^2 u_{xxt} + hh_x u_{xt} + bh^2 (u_t + g\zeta_x)_{xx}$$

$$\zeta_t + [(h+\zeta)u]_x = 0$$

where ζ denotes the surface displacement and u the vertically averaged horizontal velocity. For b=0 the momentum equation reduces to its standard form as it was derived by Peregrine [11] for a gently sloping bottom. For b=1/15 a major improvement for the dispersion characteristics is achieved. This extension to the original Boussinesq equations was first suggested by Witting [12] and then recapitulated by Madsen *et al.*[13]. A mathematical model with good dispersion characteristics is essential in this study because the waves decomposing behind the submerged obstacle generate free high frequency components which in essence may be regarded as relatively deep water waves.

In the numerical treatment of the governing equations, except for some minor but crucial adjustments, we basically followed the guidelines given in Peregrine (1967). Details of the numerical scheme will be reported elsewhere.

In figure 5a measured surface elevations are compared with the computational results for non-breaking but nonlinear random waves at selected stations. Figure 5b shows the comparisons for the measured and computed spectra at the same stations. The agreement is remarkable and justifies our choice of the governing equations.

4.3 Breaking waves

In the previous part we emphasized the overall similarity observed in the spectral evolution of breaking and non-breaking waves and substantiated it with laboratory measurements. The results clearly suggested the crucial point that for sufficiently high nonlinearity the spectral evolution for different wave conditions differed only by a scaling factor. This in turn implies that in this definite range it is possible to predict the spectral evolution of a certain wave field from the knowledge of another wave field provided that appropriate scaling is used and that the *overall* energy loss due to breaking is accounted for. This line of attack is presently in progress.

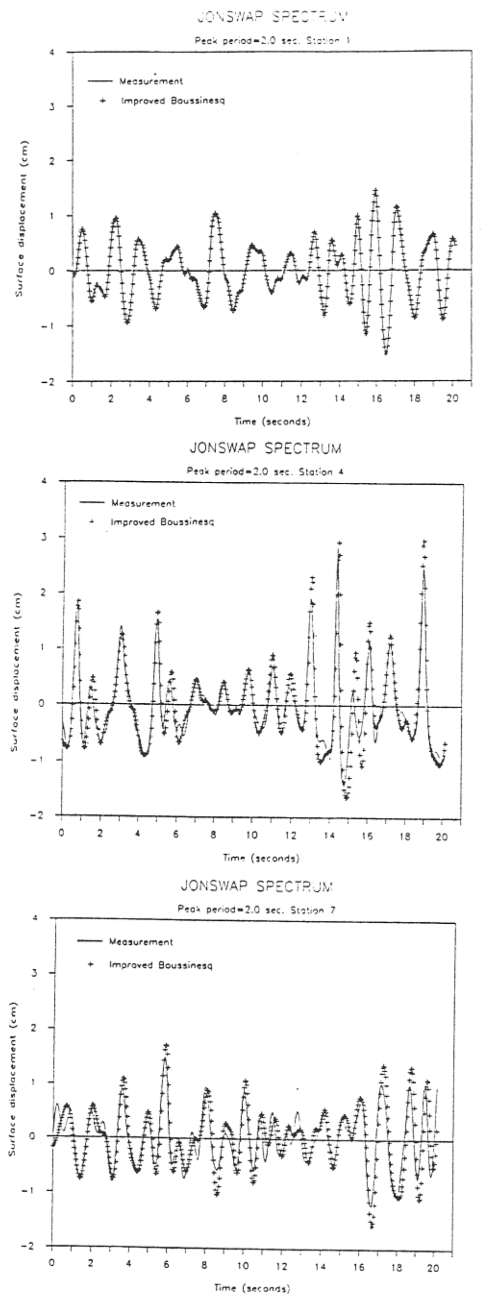

Figure 5a Time domain comparisons of measurements with numerical simulations. (f_p=0.5 Hz.)

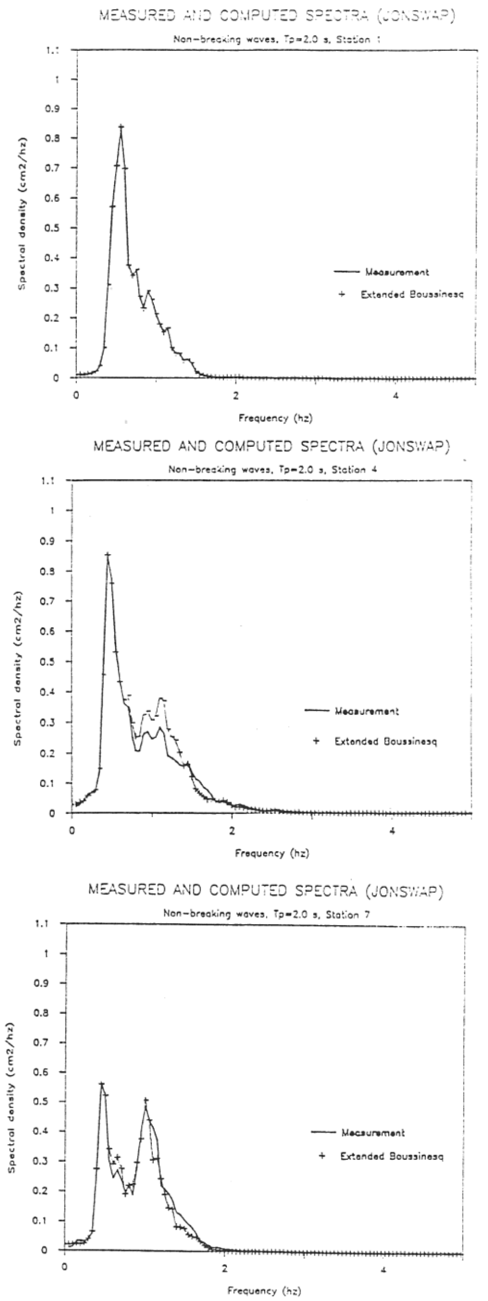

Figure 5b Spectral domain comparisons of measurements with numerical simulations. (f_p=0.5 Hz.)

5. Conclusions

Spectral and bispectral estimates computed from laboratory measurements are analyzed to clarify the effects of wave breaking on the inherently nonlinear phenomenon of high frequency energy generation and transfer in the power spectra of waves traveling over submerged profiles. It is found that wave breaking merely dissipates energy in averaged manner and does not introduce drastic alterations to the spectral shape. However it does reduce the strength of nonlinear interactions severely by *clipping* the wave heights. In this respect breaking works, as in the classical sense, as a limiting mechanism.

A practical implication of these findings is the apparent possibility of combining a weakly nonlinear non-dissipative model with a semi-empirical dissipation formulation for the total energy. This is the subject matter of ongoing research.

Acknowledgements

The software used for bispectral computations was developed by Dr. J.R.C. Doering in the course of his doctoral studies at Dalhousie University and was obtained through a personal communication. The financial support for this project was provided in part by the EC-MAST program within the framework of WASP-project.

References

[1] Mei, Chiang C., *The Applied Dynamics of Ocean Surface Waves*, World Scientific, Singapore, 1989.

[2] Phillips, O.M., On the dynamics of unsteady gravity waves of finite amplitude, Part 1. The elementary interactions, J. Fluid Mech., **9**, pp.193-217, 1960.

[3] Hasselmann, K., On the non-linear energy transfer in a gravity-wave spectrum, Part 1. General theory, J. Fluid Mech., **12**, pp.481-500, 1962.

[4] Johnson, R.S., Some numerical solutions of a variable-coefficient Korteweg-de Vries equation (with applications to solitary wave development on the shelf), J. Fluid Mech., **54**, pp.81-91, 1972.

[5] Bryant, P.J., Periodic waves in shallow water, J. Fluid Mech., **59**, pp.625-644, 1973.

[6] Sawaragi, T. and K. Iwata, On wave deformation after breaking, *Proc. of the 14th Conf. on Coastal Eng.*, ASCE, pp.481-498, 1974.

[7] Dingemans, M.W., Investigations in the undular-bore formulation, *Tech. rep.*, Part I, 68 pp., Delft Hydraulics, Delft, The Netherlands, May 1989.

[8] Ono, H., Wave propagation in an inhomogeneous inharmonic lattice, J. Phys. Soc. Jap., **32**, pp.332-336, 1972.

[9] Johnson, R.S., On the development of a solitary wave over an uneven bottom, Proc. Cambridge Philos. Soc., **73**, pp.183-203, 1973.

[10] Ohyama, T. and K. Nadaoka, Development of a numerical wave tank for analysis of nonlinear and irregular wave field, (to appear in Fluid Dynamics Res.,) 1991.

[11] Peregrine, D.H., Long waves on a beach, J. Fluid Mech., **27**, pp.815-827, 1967.

[12] Witting, J.M., A unified model for the evolution of nonlinear water waves, J. Comp. Phys., **56**, pp.203-236, 1984.

[13] Madsen, P.A., R. Murray, and O.R. Sørensen, A new form of the Boussinesq equations with improved linear dispersion characteristics, Coastal Eng., **15-4**, pp.371-388, 1991.